Journal of Applied Electrochemistry **32**: 123–128, 2002.

Aluminium composite coatings containing micrometre and nanometre-sized particles electroplated from a non-aqueous electrolyte

J. FRANSAER[1,*], E. LEUNIS[1], T. HIRATO[2] and J-P. CELIS[1]
[1]*Katholieke Universiteit Leuven, Dept. MTM, Kasteelpark Arenberg 44, B-3001 Leuven, Belgium*
[2]*Kyoto University, Department of Materials Science and Engineering, 606-8501 Kyoto, Japan*
*(*author for correspondence, e-mail: Jan.Fransaer@mtm.kuleuven.ac.be)*

Received 16 June 2001; accepted in revised form 2 October 2001

Key words: aluminium deposition, composite plating, nonaqueous electrodeposition

Abstract

The electrolytic codeposition of micro- and nano-sized particles with aluminum from a nonaqueous electrolyte is investigated. SiC, SiO_2, Al_2O_3, TiB_2 and hexagonal BN particles were codeposited with aluminium from an $AlCl_3$/dimethylsulfone ($DMSO_2$) electrolyte. The effect of particle concentration and current density on the codeposition rate of SiO_2 with aluminium was investigated. The codeposition of the various particles with Al from $AlCl_3$:$DMSO_2$ solutions is very high. The amount of codeposited particles is Langmuir dependent on the particle concentration in the electrolyte. In contrast, the effect of the current density on the amount of codeposited SiO_2 is small.

1. Introduction

Nano-structured materials are being investigated in the search for materials with new and better functional properties. One recent example is the electrodeposition of nano-crystalline copper foils exhibiting superplasticity during cold deformation at room temperature [1]. A second example is the plasma spraying of nano-structured cermet coatings with interesting friction and wear properties [2]. The availability of nano-sized powders and the interest in metallic coatings containing particles has led to research on the structuring of thin films with the help of nano-sized powders. Possible applications are dispersion strengthened thin films of interest for micro-electromechanical components (MEMS), and coatings with enhanced corrosion and wear resistance [3].

One possible way of nano-structuring is by electrolytic codeposition in which metallic, ceramic or polymeric particles suspended in an electrolyte containing metal ions, are embedded in the metal deposit resulting from the electrochemical reduction of the metal ions at the cathode. Composite coatings containing micrometre-sized particles made by codeposition are widely used in the automotive industry (e.g., wear resistant Ni–SiC coatings on aluminium motor engines) and in the aeronautics (e.g., oxidation resistant NiCo–Cr_2O_3 coatings on turbine blades). The development of composite plating with nano-sized particles is however hampered by the following two problems. In aqueous plating electrolytes, particles easily agglomerate due to the compression of the diffuse double layer surrounding the particles by the high ionic strength. This effect is more pronounced for particles of submicrometre size (i.e., $<10^{-6}$ m) as the shearing forces on the agglomerates, created by the agitation of the plating bath, decreases with particle size. As a consequence, the codeposition of agglomerated particles takes place and the anticipated mechanical, chemical and/or physical properties of the composite coatings are not reached. Secondly, the codeposition of particles decreases with particle size. The volume percent of codeposited particles in aqueous electrolytes drops from 5–15 vol % for micrometre-sized particles to 0.1 vol % or less for submicrometre-sized particles.

From recent work, there is a strong suspicion that the codeposition of non-Brownian particles from aqueous solutions is governed to a large extent by the hydration force [4, 5]. By measuring the adhesion force between a particle and an electrode, it was found that codeposition is governed by the DLVO interactions plus an additional short-range repulsion. This force was tentatively identified as the hydration force [4]. This would explain why highly hydrophilic materials such as oxides, have a small tendency to codeposit, while hydrophobic materials such as plastics, graphite, etc. codeposit readily. For instance, we have recently shown that decreasing the hydrophilicity of particles is an effective way to enhance the codeposition of particles from aqueous electrolytes [6]. Hence, the use of non-aqueous electrolytes where water is absent should allow the codeposition of strongly hydrophilic particles like SiO_2. In an attempt to overcome the problems of agglomeration of submicrometre and nanometre-sized particles and their

low degree of codeposition linked to the surface hydrophobicity, we explored the electrolytic codeposition of particles from a non-aqueous aluminium electrolyte in this work.

Electrodeposition of aluminium is possible from an $AlCl_3$–NaCl molten salt [7]. The attractiveness of this molten salt is linked to its low cost and a reasonably low working temperature (120 °C and higher). The drawbacks of the $AlCl_3$–NaCl molten salt are its high $AlCl_3$ vapour pressure and the fact that the melt is very corrosive. Non-aqueous, solvent-based electrolytes are an alternative. In this work, an $AlCl_3$/dimethylsulfone ($DMSO_2$) electrolyte with a melting temperature of 109 °C, and a density of 1.13 g cm^{-3} was used [8–14]. This electrolyte has a much lower $AlCl_3$ vapour pressure as compared to the $AlCl_3$–NaCl molten salt and a reasonable cost (about 73 US$ per kg for high purity products). Also, this electrolyte yields good deposits and the operating temperature is reasonable.

2. Experimental details

Aluminium chloride (Fluka, $\geqslant$99% purity) was used in the as-received state. Dimethylsulfone (Fluka, $\geqslant$98% purity) was dried at 60 °C for 6 h in a glove box filled with dry nitrogen. The nitrogen was circulated through a drying train (relative humidity at room temp. $\leqslant$1.5%). Electrolytes were prepared by mixing 150 g of $DMSO_2$ with 42.2 g of $AlCl_3$ and the appropriate amount of particles in a glass deposition cell inside the glove box. This composition corresponds to a ratio of 2 mol $AlCl_3$ for 10 mol $DMSO_2$. The cell was hermetically closed with a double walled lid and the $AlCl_3$–$DMSO_2$ electrolyte was subsequently heated by circulating silicone oil through the double wall of the glass vessel. All handling of the electrolyte and the deposition are done inside the glove box to prevent oxidation and water uptake by the electrolyte. Five types of particles were selected: SiC with a mean particle size of 700 nm (Elektroschmelzwerk Kempten, Germany), monodisperse, spherical SiO_2 particles of 200 nm (Geltech, USA), polydisperse, spherical Al_2O_3 particles with a mean size of 50 nm (Plasmachem, Germany), TiB_2 with a mean particle size of 1.9 μm (Elektroschmelzwerk Kempten, Germany) and finally, hexagonal BN platelets with a mean size of 4 μm (H.C. Starck, Germany). The particles were dried at 200 °C for 24 h before addition to the electrolyte. The concentration of particles in the plating bath was 53 g l^{-1} except for the BN where the concentration was 38 g l^{-1}. The particles were kept in suspension in the plating bath by a magnetic stirring rod encased in borosilicate glass.

Aluminium rods (99.995% purity) were used as anode and reference electrode. The cathode was a copper block shaped with cylindrical ends and a round cross section with a diameter of 5 mm. Before metal deposition, the cathode was polished, degreased, rinsed with distilled water, thoroughly air dried and covered with PTFE tape to expose only one end to the solution. For electrical contact, the copper cathode was connected to a copper rod covered with PTFE tape, and the surface on which aluminum deposited was positioned vertically, facing the anode. Copper sputtered silicon wafers were used as cathode to observe fractured cross sections. The samples for the chemical analysis were deposited on copper substrates with a diameter of 10 mm mounted in a holder made out of PEEK. After mechanical polishing, the samples were electrolytically polished in a propanol, butanol and phosphoric acid mixture, rinsed in alcohol and water and dried. During deposition, the samples were facing downwards.

All codeposition experiments were performed at 110 °C. This is the lowest temperature at which electrolysis can be performed with this electrolyte. The electrodepositions were done galvanostatically. The current density was 13 A dm^{-2} for the initial 20 s, and changed to the effective plating current densities thereafter. The total electrical charge was kept constant at 7500 C dm^{-2}, corresponding to a theoretical thickness of 25 μm.

After electroplating at constant current, the electrodeposited coatings were investigated using a scanning electron microscope (Philips XL30-FEG) equipped with EDX elemental analysis. The deposits were rinsed after deposition, in propylene carbonate at 40 °C in a glove box. After the samples were taken out of the glove box, they were rinsed in distilled water at 60 °C and in ethanol, and dried. Ultrasonic cleaning in water was applied for 10 min twice on each sample to remove loosely adsorbed particles from the surface.

3. Results and discussion

SEM pictures of the surface morphology of as-plated composite aluminium coatings electroplated from the $AlCl_3$–$DMSO_2$ electrolyte are shown in Figures 1 to 5 for the different types of particles selected in this study. Dense and smooth aluminium deposits are obtained in all cases and the growth morphology of the aluminium matrix is not affected by the particles. The angular SiC particles can easily be differentiated from the aluminium matrix by their shape (Figure 1). The different stages of the codeposition of SiO_2 particles evolving from particles adsorbed on top of the coating to particles almost completely engulfed in the aluminum matrix can be seen in Figure 2. The codeposited alumina particles are more difficult to recognize due to their polydispersity, their small size (50 nm) and spherical geometry. The Al_2O_3 particles can be seen in Figure 3 as slightly brighter spheres protruding from the coating. Further proof of the presence of alumina particles in the composite aluminium layers comes from the high amounts of oxygen found in EDX analyses of the Al–Al_2O_3 coatings. Also, the irregularly shaped TiB_2 particles codeposit easily with aluminum from the non-aqueous $DMSO_2$ electrolyte (Figure 4). In Figure 5, the BN

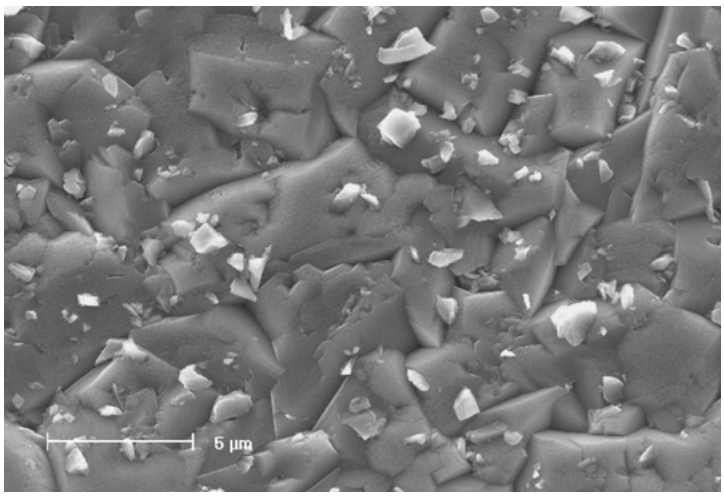

Fig. 1. Surface morphology of as-plated composite Al–SiC coatings obtained from a $AlCl_3$–$DMSO_2$ electrolyte operated at 110 °C, 8 A dm^{-2} and containing 53 g l^{-1} 700 nm SiC particles.

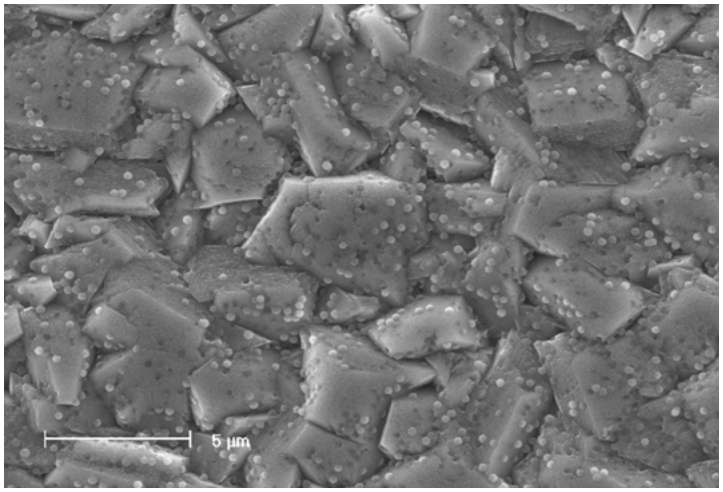

Fig. 2. Surface morphology of as-plated composite Al–SiO_2 coatings obtained from a $AlCl_3$–$DMSO_2$ electrolyte operated at 110 °C, 13 A dm^{-2} and containing 53 g l^{-1} monodisperse 200 nm spherical SiO_2 particles.

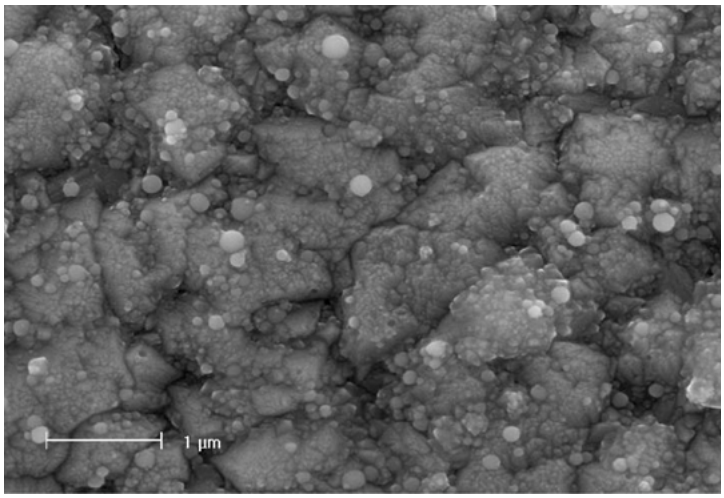

Fig. 3. Surface morphology of as-plated composite Al–Al_2O_3 coatings obtained from a $AlCl_3$–$DMSO_2$ electrolyte operated at 110 °C, 8 A dm^{-2} and containing 53 g l^{-1} spherical Al_2O_3 particles with a mean size of 50 nm.

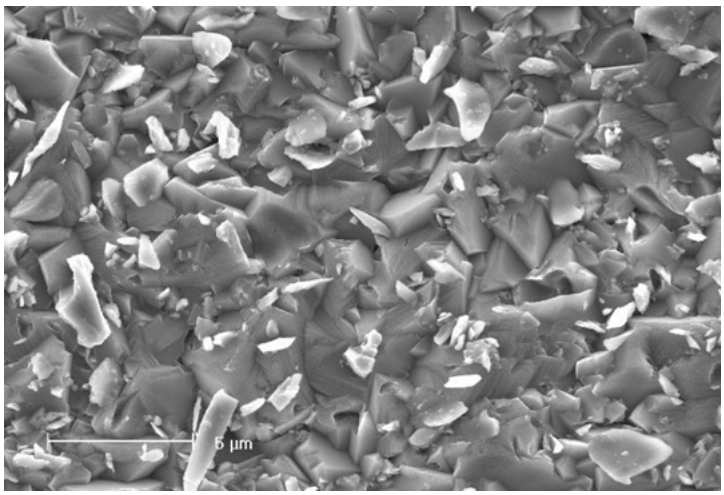

Fig. 4. Surface morphology of as-plated composite Al–TiB_2 coatings obtained from a $AlCl_3$–$DMSO_2$ electrolyte operated at 110 °C, 8 A dm^{-2} and containing 53 g l^{-1} 1.9 μm sized TiB_2 particles.

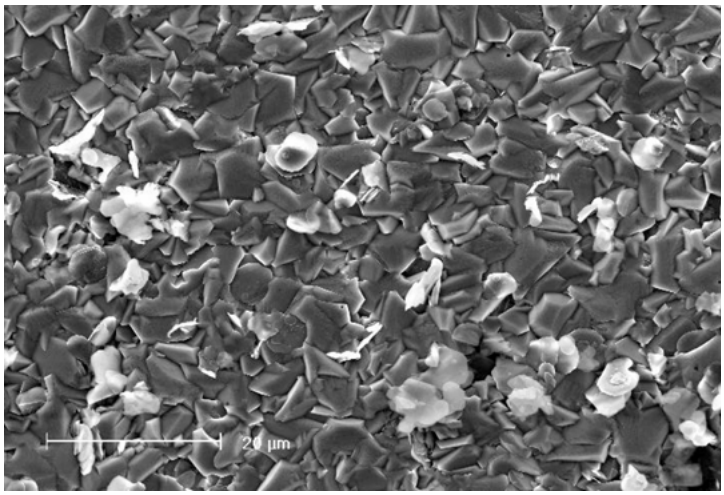

Fig. 5. Surface morphology of as-plated composite Al–BN coatings obtained from a $AlCl_3$–$DMSO_2$ electrolyte operated at 110 °C, 8 A dm^{-2} and containing 38 g l^{-1} 4 μm BN particles.

particles are the white platelets that stick out from the coatings. The amount of codeposited BN is lower than in the previous Figures but this is due in part to the fact that the concentration of BN in the electrolyte was lower (38 g l^{-1} against 53 g l^{-1}). All of the investigated particles codeposit with aluminium, some of them in high concentration. This is remarkable since some of these particles hardly codeposit from aqueous plating baths (e.g., SiO_2). Also, the particles codeposited as individual particles as no agglomerates can be seen on the surface of any of the composite coatings produced from this non-aqueous electrolyte. Figure 6 shows a SEM image of a fractured cross section of a composite Al–SiO_2 layer deposited on a copper sputtered silicon wafer. The electrodeposition was done at 8 A dm^{-2} corresponding to an experimentally determined growth rate of the aluminum matrix of about 77 μm h^{-1}. In this 20 μm thick aluminium coating, the SiO_2 particles are homogeneous embedded as individual particles over the whole cross-section. This proves the SiO_2 particles cannot only be seen on top of the coating but are also present in the bulk of the coating.

For the Al–SiO_2 system, the effect of particle concentration and current density on the rate of codeposition was investigated (Figures 7 and 8) by inductively coupled plasma atomic emission spectroscopy (ICP–AES). After deposition, the coatings were detached from the substrate, weighted and dissolved in a mixture of phosphoric acid and nitric acid at 250 °C. The concentration of SiO_2 in the aluminium coatings was determined by ICP–AES from the strength of the Si emission line. The data shown in Figures 7 and 8 are the average of three different samples and the error bars correspond to $\pm 3\sigma$. Figure 7 shows the concentration (in volume percent) of silica particles in Al–SiO_2 coatings obtained from a 2:10 $AlCl_3$–$DMSO_2$ electrolyte operated at 110 °C, at 11 A dm^{-2} as a function of the particle concentration in the electrolyte. As can be seen, the codeposition increases almost linearly with particle concentration up to 20 g l^{-1}. Particle concentrations in

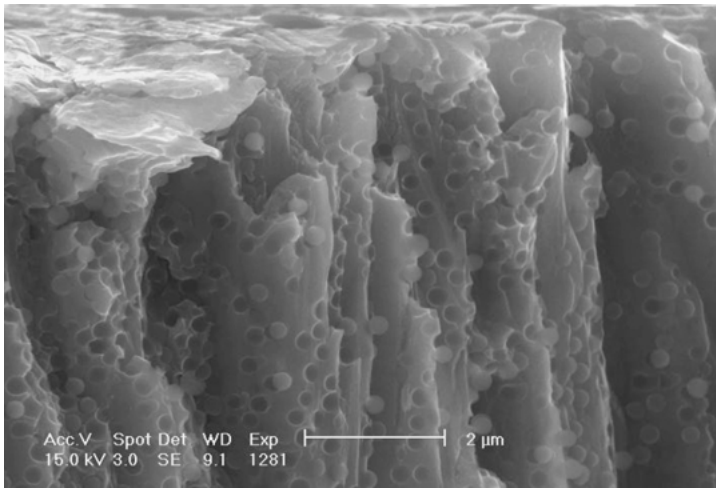

Fig. 6. Fractured cross section of a composite Al–SiO_2 coating obtained from a $AlCl_3$–$DMSO_2$ electrolyte operated at 110 °C, 8 A dm^{-2} and containing 53 g l^{-1} 200 nm SiO_2 particles.

the plating bath higher than 20 g l^{-1} do not bring about a further increase in the amount of codeposited particles and the codeposition saturates at 12 vol % of SiO_2 in the coating. The data of Figure 7 was fitted by a Langmuir adsorption isotherm (dashed line):

$$c_{\text{coating}} = \frac{\alpha\beta c_{\text{bath}}}{1 + \beta c_{\text{bath}}}$$

where c_{coating} and c_{bath} are the particle concentration in the coating and plating bath, and α and β are constants. In the original formula derived by Langmuir, α equals 1 since the whole surface is equiaccessible to molecules and β is related to the difference in energy for the adsorption and desorption process of gas molecules on solid surfaces. For the fit in Figure 7, α and β equal 0.11 and 13.5, respectively. The value of α corresponds to the particle concentration in the coating for high bath loadings, while $\alpha\beta$ is the slope of the graph at low bath loadings. The fact that α is substantially smaller than 1 indicates that the particles on the surface hinder the approach of newly arriving particles. As in the original formula by Langmuir, we believe that β is related to the strength of the interaction between particles and electrode. As can be seen in Figure 7 and as noted earlier by Guglielmi [15], the Langmuir adsorption isotherm fits the codeposition data very well. This Langmuir behaviour of the amount of codeposited particles on the concentration of particles in the plating bath is typical for codeposition. The Langmuir dependence has to do

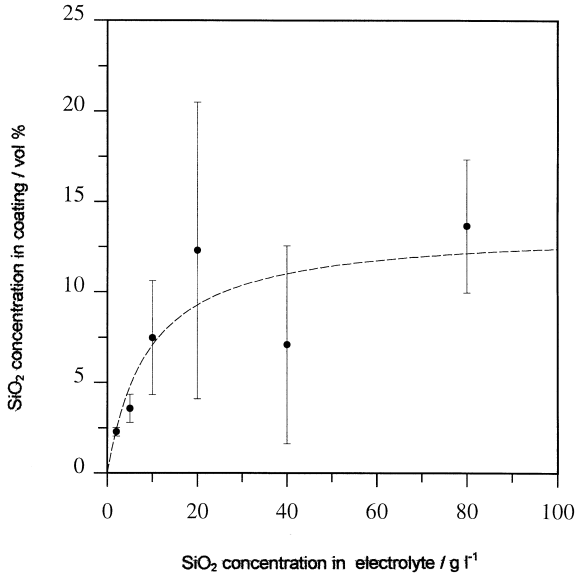

Fig. 7. Concentration (in volume percent) of 200 nm silica particles in Al–SiO_2 coatings obtained from a 2:10 $AlCl_3$–$DMSO_2$ electrolyte operated at 110 °C, at 11 A dm^{-2} as a function of the particle concentration in the electrolyte in g l^{-1}. Key: (●) experimental plot; (- - - -) Langmuir isotherm.

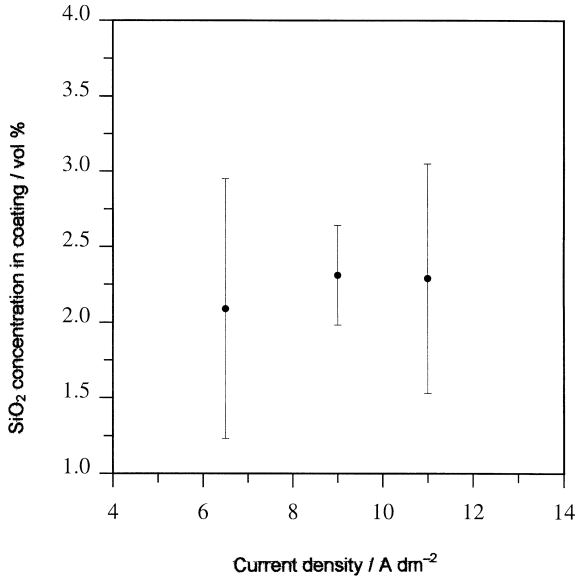

Fig. 8. Concentration of silica particles in Al–SiO_2 coatings obtained from a 2:10 $AlCl_3$–$DMSO_2$ electrolyte with 2 g l^{-1} of 200 nm SiO_2 particles operated at 110 °C, as a function of the current density in A dm^{-2}. Key: (●) experimental plot.

primarily with the mass transport of particles to the surface of the cathode and is hence independent of the nature of the plating bath. The value of the saturation limit is due to surface blocking effects for small particles and hydrodynamic shielding for bigger particles.

The concentration of silica particles in Al–SiO_2 coatings obtained from a 2:10 $AlCl_3$–$DMSO_2$ electrolyte with 2 g l^{-1} of particles operated at 110 °C, as a function of the current density can be found in Figure 8. In these experiments, the current was varied between 6.5 and 11 A dm^{-2}. Lower and higher current densities could not be used since either bad coatings were produced or the coating quality was no longer uniform. This Figure shows that, within this current density range, the amount of codeposited particles varies very little with current density and that up to 2 vol % of silica particles can be codeposited from a plating bath with 2 g l^{-1} of silica. This is attractive from a technological point of view since high rates of codeposition can be achieved from non-aqueous electrolytes containing low amounts of suspended particles (less than 10 g l^{-1}). This is in contrast to composite plating from aqueous electrolytes that requires high amounts of suspended particles to achieve a reasonable degree of codeposition (typically in the range of 50 to 200 g l^{-1} for micrometre-sized particles).

4. Conclusions

This introductory investigation demonstrates that the codeposition of micrometre and nanometre-sized particles is possible from non-aqueous electrolytes. The large degree of codeposition of hydrophilic particles (SiO_2 and Al_2O_3) confirms that elimination of the hydration force achieved by using non-aqueous electrolytes, can significantly enhance the codeposition of such particles and can avoid the agglomeration that takes place in aqueous electrolytes. This opens new fields of applications for the synthesis of composite coatings containing homogeneously dispersed nanometre-sized particles with compositions that cannot be obtained from aqueous electrolytes.

Acknowledgements

This work was funded in part by the FWO-Vlaanderen (contracts G.0337.98 and G.0299.99) and by the Belgian Government (contract IUAP 4/33). JF thanks the FWO-Vlaanderen and TH thanks the Japanese Science Foundation as their respective funding sources. EL and JF wish to thank G. Stafford (NIST) for his generous help in starting up this research. The authors thank J. Van Dyck for his help with the ICP analysis.

References

1. L. Lu, M.L. Sui and K. Lu, *Science* **287**(2) (2000) 1463–1466.
2. B.H. Kear and G. Skandan, *Nanostruc. Mater.* **8**(6) (1997) 765–769.
3. I. Garcia Diego, J. Fransaer, and J-P. Celis, to appear in Wear (2001)
4. J. Fransaer, J-P. Celis and J.R. Roos, *J. Electrochem. Soc.* **139** (1992) 413–425.
5. C. Dedeloudis, J. Fransaer and J-P. Celis, *J. Phys. Chem.* **104** (2000) 2060–2066.
6. V. Terzieva, J. Fransaer and J-P. Celis, *J. Electrochem. Soc.* **147** (2000) 198–202.
7. G. Stafford, *J. Electrochem. Soc.* **136** (1989) 635–639.
8. L. Legrand, M. Heintz, A. Tranchant, and R. Messina, *Electrochim. Acta* **40** (1995) 1711–1716.
9. J.P. Pereira-Ramos, R. Messina and J. Perichon, *J. Electroanal. Chem.* **209** (1986) 283–296.
10. L. Legrand, A. Tranchant, and R. Messina, *Electrochim. Acta* **39** (1994) 1427–1431.
11. L. Legrand, A. Tranchant, and R. Messina, *J. Electrochem. Soc.* **141** (1994) 378–382.
12. L. Legrand, A. Tranchant, and R. Messina, F. Romain and M. Lautie, *Inorg. Chem.* **35** (1996) 1310–1312.
13. L. Legrand, A. Tranchant, and R. Messina, *Electrochim. Acta* **41** (1996) 2715–2720.
14. T. Hirato, J. Fansaer, J-P. Celis, *J. Electrochem. Soc.* **148** (2001) C280–C283.
15. N. Guglielmi, *J. Electrochem. Soc.* **119** (1972) 1009–1012.